Electro-Optical calibration of pupil plane modulators for pyramid WFS

Runa Briguglio[a], Fabio Rossi[a], Enrico Pinna[a], Alfio Puglisi[a], Manny Montoya[b], and Olivier Durney[b]

[a]INAF Osservatorio Astrofisico Arcetri L. E. Fermi 5, 50125 Firenze Italy
[b]Steward Observatory, Department of Astronomy, University of Arizona, 993 N. Cherry Ave, Tucson, AZ, 85721, USA

ABSTRACT

Circular pupil plane modulation enlarges the pyramid WFS linear range and reduces the static pattern due to diffraction. This technique is applied in the majority of the SCAO system with Pyramid WFS. In order to properly adjust the sensor gains, the optical modulator shall be able to produce a circle of a given amplitude at the WFS frequency. Deviations from the perfect circular pattern can produce tilt offset and sensitivity losses. We describe the automated procedure for the fine tuning of the modulator, succefully applied up to 2kHz of revolution for the SOUL WFSs at the LBT. The procedure includes the optimization for high dynamics of the piezo actuator and the optical calibration of the kinematics to produce the circular pattern at the desired amplitude, frequency and projection angle.

Keywords: Adaptive Optics, Pyramid wavefront sensors, Tiptilt modulator, piezo-electric actuators

1. INTRODUCTION: PUPIL MODULATION FOR PYRAMID WFS

Tip tilt circular modulation allows to modify the optical gain of the pyramid wavefront sensor and allows to tune the linear range of this wavefront sensor. In the figure below sensitivity and dynamic range are shown for a set of amplitudes. A robust implementation of tip tilt modulation is obtained with a steering mirror which shall be optically conjugated with the system stop (pupil). The modulation device must provide a complete revolution of the PSF around the pyramid tip in an exact exposure time of the WFS camera; also, the PSF pattern on the pyramid shall be a perfectly circular. Any deviation from circularity or desired timing is translated into an illumination un-balance on the pyramid faces and on the WFS camera, resulting is a WF offset. This is why the modulation device shall be accurately tuned before use in the WFS.

In this work we present the calibration performed on a piezo modulation device. The study case is the SOUL project[12],[3] which is the upgrade of the FLAO[1] system for 2 kHz operations. The modulator calibration included therefore the fine tuning of the modulation pattern and the optimization of the device internal control for high dynamics operations.

2. PIEZOELECTRIC ACTUATOR AS OPTICAL MODULATOR

In the following we will focus on the piezo-electric actuators we adopted for our pyramid WFS. They are manufactured by the german company Physik-Instrumente and consist of a number (3 or 4) of piezo-stack elements acting on a moving platform with a mirror. The piezo elements are bonded to the bottom part of the external housing; on the top, they are pre-compressed by the platform via a central spring: the mechanical contact between the piezo and the platform is realized by a sphere to allow the platform rotation. The pre-compression permits the piezos to work in both directions (compression and expansion). The moving platform is attached to the external housing by means of a blade-spring, featuring a very high lateral rigidity and a lower vertical one, to allow the vertical displacement requested for the rotation. The blades are arranged according to a 45 °
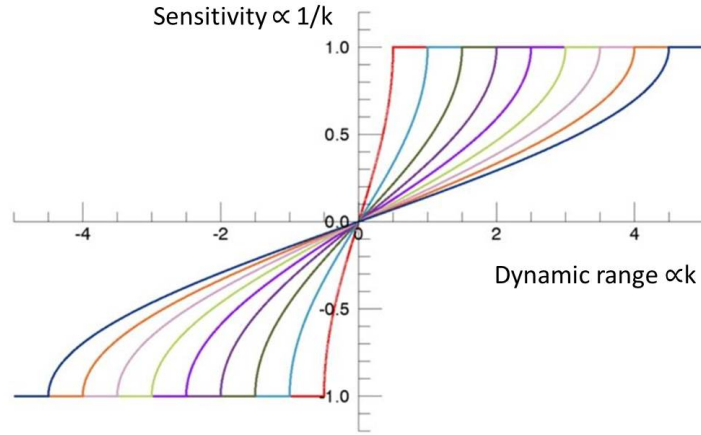

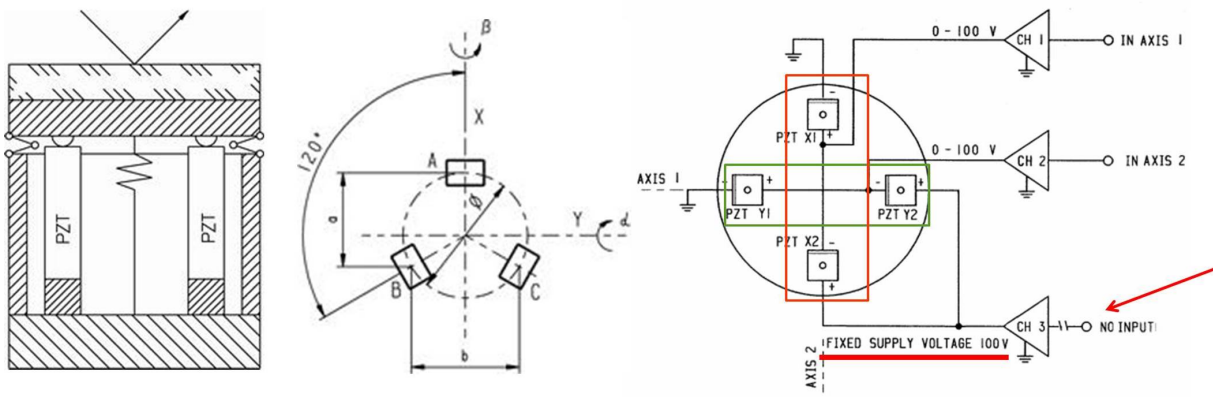Figure 1. Dynamic range plotted against sensitivity for a pyramid WFS, for various modulation amplitude

Figure 2. Left, middle: working mechanisms of the PI piezo actuators used during the tests (differential, with two axes and tripod with three axes. Right: scheme of the electrical excitation scheme for the differential actuator. Courtesy PI

symmetry and the impact of such geometry on the dynamical performances will be discussed later. The piezo stacks are equipped with a strain-gauge sensor (SGS) bonded to the side to measure the piezo expansion; the SGS reading provides the feedback for a closed control loop to regulate the piezo driving voltage.

We considered two different kinds of actuators, the SL-325 with 3 axes and the SL-330 with two axes. The SL-325 is equipped with 3 piezo elements at a 120 ° geometry and allows the application of piston and tip/tilt commands. Each piezo element is powered by a dedicated high voltage power supply. The imperfect matching between the 120 ° geometry of the piezos and the 45 ° of the blades results into a different mechanical behaviour of the three piezos. Such actuator is the one adopted for the two FLAO systems installed at the LBT on 2010. During the SOUL upgrade, the actuators have been calibrated to work at 2 kHz frequency.

During the preliminary design phase of the GMT pyramid WFS[4] we investigated and tested the SL-330 for 2 kHz modulation. Such system, differently from the SL-325, is more specifically designed for higher dynamics also thanks to a lighter moving platform. The system is equipped with 4 opposite piezo elements and a fixed central pivot point, so that tip and tilt only are allowed. The electrical connection of the piezo couple is such as the elements perform an opposite displacement for any control voltage applied.

3. CALIBRATION PROCEDURE AND RESULTS

The strategy to set-up a piezo actuator for high dynamics operation is conceptually composed by two main tasks. In a first step, using the feeback provided by the SGS, the parameters of the internal control loop are adjusted to speed-up the actuator response. In a second step, the command parameters are adjusted separately on the different axes with an external optical feedback to obtain a circular modulation pattern at a given amplitude and frequency. Such separate steps with different feedback are requested since the SGS are physically attached to the piezo-ceramic strips and not to the moving platform, which in turn is connected to the piezo via the spring force only. Especially at high frequency, the SGS measurement is therefore not a reliable measurement of the platform position. We underline here that the optical feedback shall not be at high temporal cadence, i.e. we just need to integrate on a camera a number of trajectories to measure its main parameters (radius, ellipticity, e.g.). The procedure is summarized in the following steps:

SGS feedback   1. Adjust the control loop parameters to speed up the settling time.

2. Regulate the notch filter to suppress the system oscillations.

3. Check for cross-talk among axes and equalize the responses.

Optical feedback   1. Drive the actuator with the nominal commands for a circular pattern.

2. Adjust differentially the excitation parameters (input voltage and relative phase) to improve the modulation pattern.

3. Repeat the previous steps for any control frequency and amplitude.

3.1 Fine tuning of the actuator control loop

The working scheme of the piezo driver control loop allows both for close and open loop operations, configurable with a physical switch, one per actuator. In close loop, the target position is compared to the SGS reading and processed with a gain/integrator circuit; both in close and open loop, the driver output is filtered by a slew rate limiter and a notch filter. The control loop is managed by a dedicated E-802 electronic board, one per piezo channel; the SGS reading and processing is demanded to a secondary board, one per channel as well. According to such schematization, the loop parameters that can be tuned are:

- the output voltage slew rate limiter;

- the loop gain;

- the time constant of the integrator;

- the notch filter frequency, bandwidth and slope;

- the SGS gain and offset.

Within the present work, we didnt modify the SGS calibration as we trusted in the factory ones, regulated in DC with the optical feedback of an interferometer by PI. No AC calibration of the SGS was possible with the current setup, because an imaging system with a kHz bandwidth would be required. All the parameters are adjusted by mean of potentiometers on the electronic boards. All the potentiometers provide an analogical 30-turns regulation of the associated parameter. We based our tuning procedure on the instructions provided by the manufacturer, and it consists on the comparison between the command injected on each channel and the SGS signal measured, by means of an oscilloscope. We modified the procedure according to our needs, as in the following steps.

1. remove the slew rate limiter and set the slew rate regulation potentiometer to 30 turns clockwise (full range position, corresponding to maximum slew rate);

2. select a notch filter frequency of 3kHz or higher;

3. inject a square wave command, 1V amplitude, 20-30 Hz frequency, on channel 1; check command and SGS reading on the oscilloscope;

4. regulate the loop gain potentiometer to match the SGS steady state reading with the command;

5. regulate the integrator time constant potentiometer to speed-up the settling time; define a maximum overshoot threshold;

6. regulate the notch filter to suppress the loop oscillations;

7. repeat the last steps for the other channels;

8. inject a square wave command, 1V amplitude, 20-30 Hz frequency, on all the channels with 0 degrees; check commands and SGS readings on the oscilloscope;

9. Fine-regulate the gain and the time constant on all channels to equalize the step responses.

At this point the channels are individually optimized for high speed operations and the effect on the parameters tuning is shown in the following.
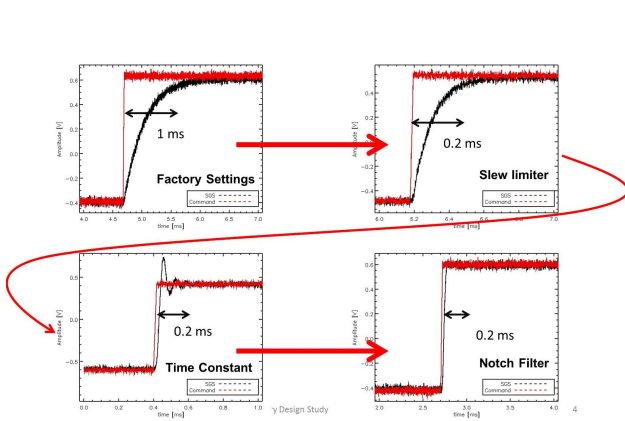

Figure 3. Single axis step response, as measured with the on-board strain gauge sensor, at the different steps of the control loop tuning.
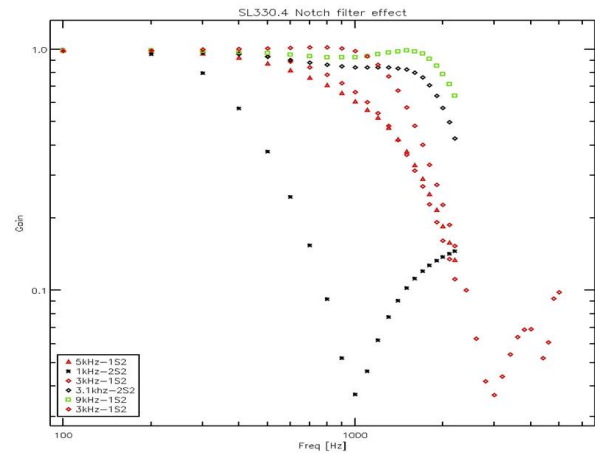

Figure 4. Single axis transfer functions for different configuration of the control loop.

3.2 Optical calibration of the modulation pattern

The optical calibration procedure allows to tune both the axes differential responses and to compensate for the modulator orientation with respect to the optical axis in order to produce a perfect circular modulation pattern. A camera shall be installed at the system focus and frames shall be captured at a frame rate slow enough to average many modulation tracks on the CCD. A configuration is given by two vectors $A = [a_1, a_2, a_3]$ and $\phi = [\phi_1, \phi_2, \phi_3]$ representing the 3 amplitudes and phases. We set as a constraint $a_2 = a_1$ and $\phi_1 = 0, \phi_2 = 120$, reducing to 3 the degrees of freedom: A_1, A_3, ϕ_3. The algorithm goal is to find the 3 parameters values such that the resulting modulation gives an ellipse of eccentricity $e < e_{max}$ and average diameter d_m such that $abs(d_m - d_{ref}) < d_{errmax}$. e_{max} and d_{errmax} are given and d_{ref} is the target modulation amplitude in pixels. Initial guess for ϕ_3 is 240 deg, while for a_1, a_3 is 1 V. For any configuration applied to the system, we can capture a frame and measure on it the resulting ellipse properties such as average diameter d_m, eccentricity e, orientation angle θ. The optical calibration steps are described in the following. Each of the steps is based on the same optimization procedure which finds the zero of an error function depending on a single parameter, implemented as a Secant Method for roots finding. In our case the function is not a known analytical one, but since we can always compute it in a given point, we can apply the method, with some cautions. In practice the error function might not have the requirements to apply such method (i.e. smoothness and existence of a single root

in the considered parameter space interval, mainly due to noise and non-linearity), so we had to include in the algorithm a termination condition allowing a limited number of steps and also limit the minimum and maximum possible values for the steps in the parameters space. Also, possible values of a_1, a_3, ϕ_3 are limited.

1. From the initial guess, optimize the amplitudes setting A to obtain the desired d. Error function: $Err(A) = d_{ref} - d_m$.

2. Optimize ϕ_3 such that the current ellipse has it major axis aligned to the Y axis. Error function: $Err(\phi_3) = $.

3. Optimize a_3 to minimize the current ellipse eccentricity. Error function: $Err(a_3) = e$.

4. Staring from the amplitudes obtained at the previous step, optimize the amplitudes by setting $A = [sa_1, sa_2, sa_3]$ to obtain the desired d. Error function: $Err(s) = d_{ref} - d_m$.

In Fig.5 we show the FLAO WFS board with the test camera for the piezo calibration added (on the bottom-left). The TTM is approximately 20° wrt to the optical axis, so that the optical calibration compensated also for the projection error. In Fig. 6 a selection of the modulation patterns obtained after the calibration is presented. The images have the same angular scale and the size corresponding to 1 mRad is indicated. What is important to note is that the high spatial frequency deviation from the circle is well within the measurement precision (the PSF of the test beam). The non-linearity of the device at the high frequencies is presented in Fig. 7 for the axis #1 (A1 voltage); also, we compare in 9 the behavior of the axis #3 versus axis #1, showing that since we are approaching a resonance frequency, specific for that axis, the required command amplitude to achieve a given displacement is lower. The relative command phase of the third axis (nominally 240 °), presented in Fig. 8 is also an indication of the resonance frequency.
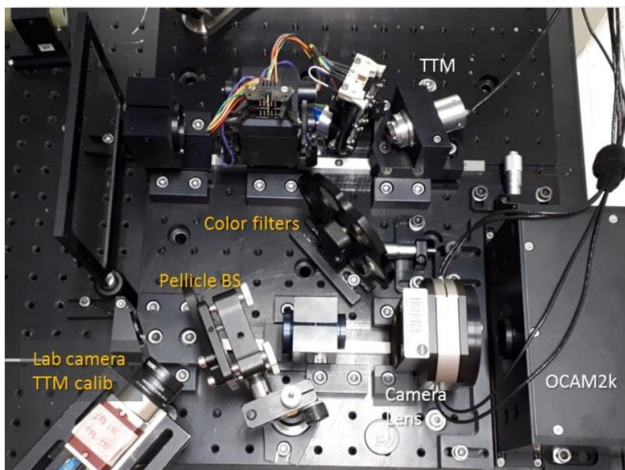

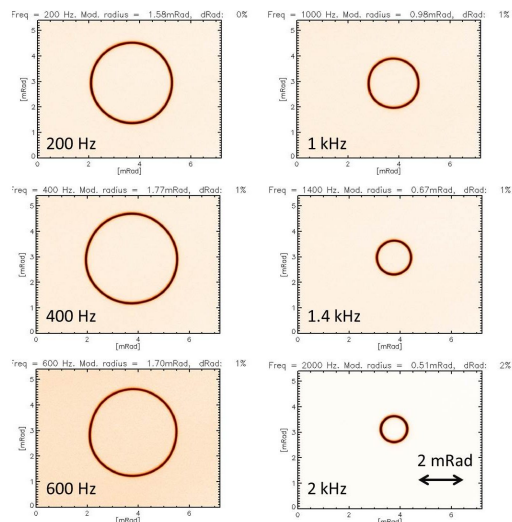Figure 5. The LBT-FLAO WFS board, placed in the optical laboratory during the SOUL upgrade.

Figure 6. Sample of modulation patterns as seen by the test camera for a number of modulation frequencies and amplitudes.

4. DISCUSSION AND CONCLUSIONS

One of the key-advantage of pyramid WFS is its variable dynamic range, thanks to the optical modulation of the PSF about the pyramid tip. The modulation is realized by a fast steering mirror, which is required to run at the same frequency of the AO loop (1 to 2 kHz) and to produce a very precise circular pattern to avoid the insurgence of WF offset. In this paper we described the calibration procedure of a piezo actuator and the results obtained: the study case is the system equipping the LBT-FLAO WFS board, upgraded during the SOUL project to work at 2 kHz. We implemented a two steps fine tuning: at first we adjusted the actuator internal control
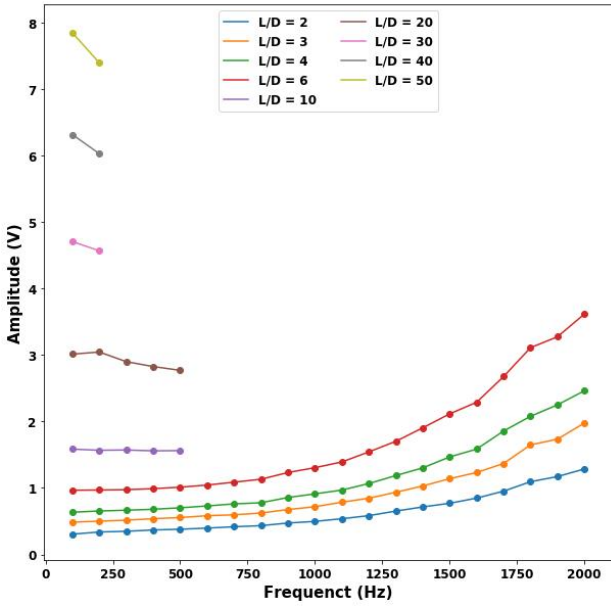
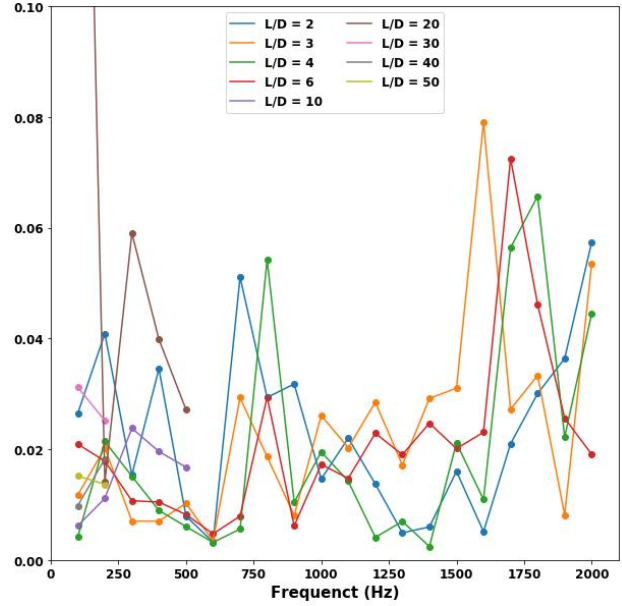Figure 7. Calibration range, frequency and command voltage.

Figure 8. Eccentricity error (min/max radius) for all the calibration runs.

loop to allow high dynamics operations; then we tuned the actuator input commands to achieve the desired modulation amplitude at a given frequency, with an optical feedback. Such a feedback allowed to compensate for the differential responses of the actuator axes also in a working regime close to the mechanical resonance. The procedure has been implemented and run on the FLAO WFS boards and in the end a complete look-up table of command voltages and differential phases has obtained for the system working points.

Acknowledgement

REFERENCES

[1] Pinna, E., Esposito, S., Hinz, P., Agapito, G., Bonaglia, M., Puglisi, A., Xompero, M., Riccardi, A., Briguglio, R., Arcidiacono, C., Carbonaro, L., Fini, L., Montoya, M., and Durney, O., "SOUL: the Single conjugated adaptive Optics Upgrade for LBT," in [*Proc. of SPIE*], *Society of Photo-Optical Instrumentation Engineers (SPIE) Conference Series* **9909**, 99093V (Jul 2016).

[2] Pinna, E., Rossi, F., Puglisi, A., and al., "Bringing SOUL on sky," in [*Proceedings of the AO4ELT6 Conference, Quebec*], (2019).

[3] Rossi, F., Puglisi, A., Pinna, E., and Grani, P., "Software solutions for high performance AO in the SOUL project," in [*Proceedings of the AO4ELT6 Conference, Quebec*], (2019).

[4] Bouchez, A. H., Acton, D. S., Agapito, G., Arcidiacono, C., Bennet, F., Biliotti, V., Bonaglia, M., Briguglio, R., Brusa-Zappellini, G., Busoni, L., Carbonaro, L., Codona, J. L., Conan, R., Connors, T., Durney, O., Espeland , B., Esposito, S., Fini, L., Gardhouse, R., Gauron, T. M., Hart, M., Hinz, P. M., Kanneganti, S., Kibblewhite, E. J., Knox, R. P., McLeod, B. A., McMahon, T., Montoya, M., Norton, T. J., Ordway, M. P., D'Orgeville, C., Parcell, S., Piatrou, P. K., Pinna, E., Price, I., Puglisi, A., Quiros-Pacheco, F., Riccardi, A., Roll, J. B., Trancho, G., Uhlendorf, K., Vaitheeswaran, V., van Dam, M. A., Weaver, D., and Xompero, M., "The Giant Magellan Telescope adaptive optics program," in [*Proc. of SPIE*], *Society of Photo-Optical Instrumentation Engineers (SPIE) Conference Series* **8447**, 84471I (Jul 2012).
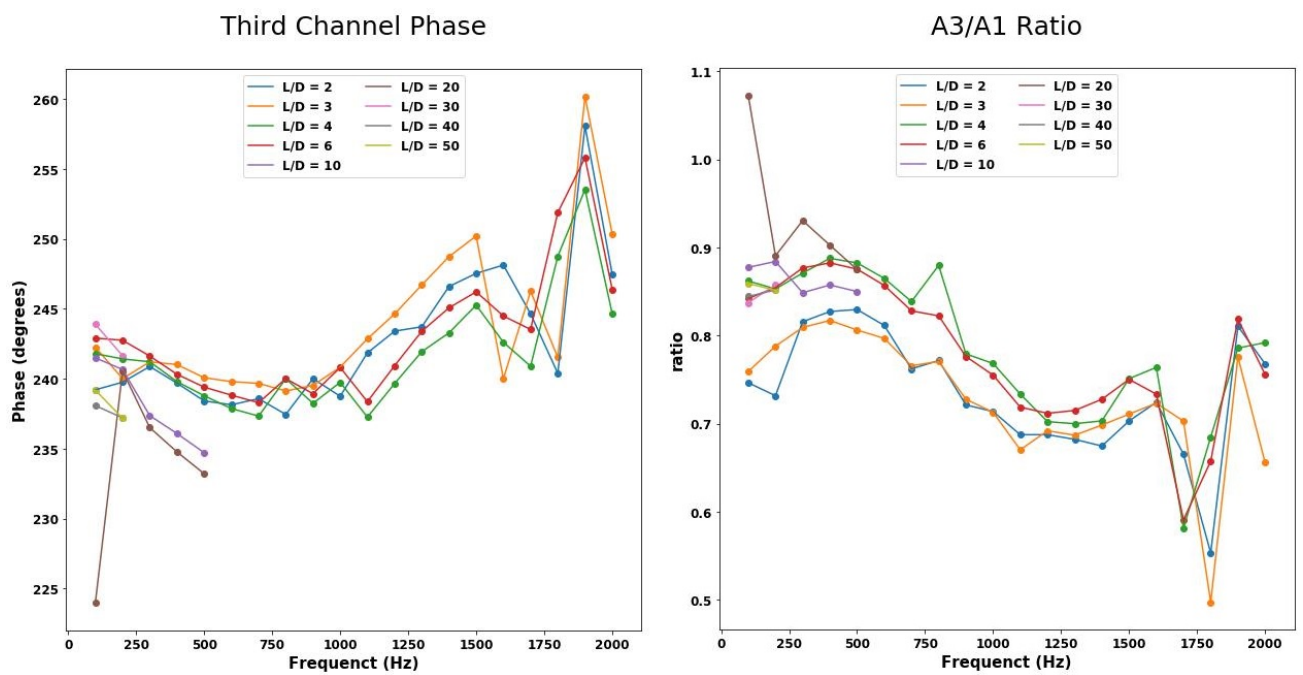
Figure 9. Differential behavior of channel 3, wrt nominal: delta phase (left) and command amplitude ratio (right). The differences take into account both the mechanical behaviour and the modulation projection due to angle of incidence on the mirror.